

PAPER

## Impact of detuning and dephasing on a laser-corrected subnatural-linewidth single-photon source

To cite this article: J C López Carreño *et al* 2019 *J. Phys. B: At. Mol. Opt. Phys.* **52** 035504

View the [article online](#) for updates and enhancements.



**IOP | ebooks™**

Bringing you innovative digital publishing with leading voices to create your essential collection of books in STEM research.

Start exploring the collection - download the first chapter of every title for free.

# Impact of detuning and dephasing on a laser-corrected subnatural-linewidth single-photon source

J C López Carreño<sup>1,2</sup> , E Zubizarreta Casalengua<sup>2</sup> , F P Laussy<sup>1,3</sup>  and E del Valle<sup>2</sup> 

<sup>1</sup>Faculty of Science and Engineering, University of Wolverhampton, Wulfruna St., Wolverhampton WV1 1LY, United Kingdom

<sup>2</sup>Departamento de Física Teórica de la Materia Condensada, Universidad Autónoma de Madrid, E-28049, Madrid, Spain

<sup>3</sup>Russian Quantum Center, Novaya 100, 143025 Skolkovo, Moscow Region, Russia

E-mail: [elena.delvalle.reboul@gmail.com](mailto:elena.delvalle.reboul@gmail.com)

Received 26 September 2018, revised 21 November 2018

Accepted for publication 5 December 2018

Published 8 January 2019



CrossMark

## Abstract

The elastic scattering peak of a resonantly driven two-level system has been argued to provide narrow-linewidth antibunched photons. Although independent measurements of spectral width on the one hand and antibunching, on the other hand, do seem to show that this is the case, a joint measurement reveals that only one or the other of these attributes can be realised in the direct emission. We discuss a scheme which interferes the emission with a laser to produce simultaneously single photons of subnatural linewidth. In particular, we consider the effect of dephasing and of the detuning between the driving laser and/or the detector with the emitter. We find that our scheme brings such considerable improvement as compared to the standard schemes as to make it the best single-photon source in terms of all-order multi-photon suppression by several orders of magnitudes. While the scheme is particularly fragile to dephasing, its superiority holds even for subnatural-linewidth emission down to a third of the radiative lifetime.

Keywords: resonance fluorescence, qubit, single-photon source, squeezing, homodyne interference, antibunching, light–matter interaction

(Some figures may appear in colour only in the online journal)

## 1. Introduction

Single photon sources lie at the heart of the quantum technologies, being fundamental for a myriad of application including quantum key distribution [1], quantum cryptography [2–4], secure direct quantum communication [5], quantum state amplification [6–8], or boson sampling [9–13]. Of the many schemes to implement a single-photon source [13–33], various strategies can be adopted to favour one or the other of its desirable characteristics, ranging from its size and ability to interface with other optical devices [14–17], its brightness [18–24], the indistinguishability between successive photons [24–30] and, of course, its sub-Poissonian character [13, 31]. To give a concrete example, one can

choose to favour indistinguishability between successive photons rather than their sub-Poissonian character [34]. More exotic schemes have also been proposed, such as the photon blockade, in both its conventional [35, 36] and unconventional [37–39] versions (both of which have been recently demonstrated experimentally [40–43]) or the heralding of single photons from two-level systems driven in Mollow triplet regime [44], let alone sources of  $N$ -photons ‘bundles’ [45, 46]. One of the most popular platforms for the generation of single photons, both from an experimental and theoretical point of view, is a two-level system. This can be realised in a variety of platforms ranging from cold atoms [47–49], to semiconductor quantum dots [25, 50–57] passing by ions [58–60], molecules [61–64], superconducting circuits

[65–69], nitrogen vacancies [70, 71], semiconductor nanocrystals [72], among others. A priori, a two-level system fits perfectly the purpose, as it can only sustain a single excitation at any given time. Thus, its repetition rate is limited by the time it takes to ‘reload’, and one can expect a perfectly antibunched emission. This is however a simplified description that ignores a central aspect of quantum theory: the detection process. The two-level system is characterized to the best of its abilities only by a detector that can measure its emission with infinite precision in time. Conversely, if the detector has a finite temporal resolution (as is of course the case in any actual setup), or, equivalently, a finite bandwidth, the theoretically perfect suppression of the second-order correlation function is spoiled by the Heisenberg uncertainty principle [73]. This can be described accurately by the theory of frequency-filtered correlations [74].

While the impact of detection is a fundamental principle that applies to all quantum systems, an interesting and somehow counter-intuitive effect occurs when turning to the detected emission of a two-level system driven coherently in the so-called Heitler regime [75], in which the emission of a two-level system consists of two components: (i) photons that are absorbed and later re-emitted (fluorescence) and (ii) photons that are elastically scattered by the two-level system (in a coherent absorption and re-emission process). The former are emitted with a Lorentzian profile centred at the frequency of the driving laser (assuming resonance with the two-level system) and with the natural linewidth of the two-level system, constituting the incoherent fraction of the emission. The latter are emitted as a  $\delta$ -narrow peak (assuming a vanishing linewidth for the laser), which forms the coherent fraction of the emission that dominates at low driving. Like any two-level system, the total emission is antibunched. The idea then arose to use the  $\delta$  peak to collect antibunched photons with narrow spectral width [76, 77]. Here as well, one must not forget the process of detection, and taking it into account, we have shown that these two qualities are not realised jointly [33]: the detected photons are either antibunched, but with a spectral width no better than that of the emitter itself, or they can be detected with the spectral bandwidth of the  $\delta$  peak, but then their antibunching is dramatically reduced. Interestingly, however, we have shown in the same work [33] how to detect photons jointly with a subnatural linewidth and an excellent antibunching, by interfering the emission of the filtered two-level system with an external laser. This laser correction removes, through destructive interferences, the excess of coherent emission when focusing on the  $\delta$  peak, in a process akin to an homodyne interference [78, 79]. Similar schemes have been recently implemented to obtain a source of indistinguishable photons [27], to observe the rising of the so-called dynamical Mollow triplet [80] and to unveil the photon correlations of the light emitted by a Jaynes–Cummings system [81]. In our case, we find that not only this laser-correction allows to realise simultaneously subnatural linewidth spectral emission and antibunching, but also that it produces a stronger type of single-photon emission with a plateau in the time-resolved photon correlation  $g_a^{(2)}(\tau)$ . Such sources therefore provide a

new playground of their own, whose properties, advantages over existing sources and further possibilities deserve an immediate attention, as we wait for their experimental implementation.

In this text, we provide a more general picture, including other interesting features of the statistics, such as perfect superbunching (where, to first order in the driving,  $g_a^{(2)}(0)$  becomes infinite) in addition to the previously reported perfect antibunching ( $g_a^{(2)}(0) = 0$ ). More particularly, we focus on the effect of two important aspects not considered previously: the impact of dephasing, since this is a detrimental ingredient that is typically present, especially in a solid-state platform, and the role of detuning from the two-level system, from either the driving laser and/or the detector.

## 2. Theoretical description

We consider a two-level system driven by a coherent source in the regime of low excitation, commonly referred to as the Heitler regime, with Hamiltonian (we take  $\hbar = 1$  along the text)

$$H_\sigma = (\omega_\sigma - \omega_L)\sigma^\dagger\sigma + \Omega_\sigma(\sigma^\dagger + \sigma). \quad (1)$$

The two-level system has a frequency  $\omega_\sigma$  and is described through an annihilation operator  $\sigma$  that follows the pseudo-spin algebra, whereas the laser is treated classically, i.e. as a  $c$ -number, with intensity  $\Omega_\sigma$  and frequency  $\omega_L$ . The dissipative character of the system is included in the dynamics through a master equation

$$\partial_t \rho = i[\rho, H_\sigma] + \frac{\gamma_\sigma}{2}\mathcal{L}_\sigma\rho + \frac{\gamma_\phi}{2}\mathcal{L}_{\sigma^\dagger\sigma}\rho, \quad (2)$$

where  $\gamma_\sigma$  is the decay rate of the two-level system,  $\gamma_\phi$  is the dephasing rate,  $H_\sigma$  is the Hamiltonian in equation (1) and  $\mathcal{L}_\sigma\rho = 2\sigma\rho\sigma^\dagger - \sigma^\dagger\sigma\rho - \rho\sigma^\dagger\sigma$ . The steady-state solution of equation (2) can be written in terms of two magnitudes: the population,  $\langle\sigma^\dagger\sigma\rangle \equiv n_\sigma$ , and the coherence,  $\langle\sigma\rangle \equiv \alpha$ , of the two level system:

$$\rho_{ss} = \begin{pmatrix} 1 - n_\sigma & \alpha \\ \alpha^* & n_\sigma \end{pmatrix}, \quad (3)$$

where

$$n_\sigma = \frac{4(\gamma_\sigma + \gamma_\phi)\Omega_\sigma^2}{\gamma_\sigma[(\gamma_\sigma + \gamma_\phi)^2 + 4\Delta_\sigma^2] + 8(\gamma_\sigma + \gamma_\phi)\Omega_\sigma^2}, \quad (4a)$$

$$\alpha = \frac{2i\gamma_\sigma\Omega_\sigma[2i\Delta_\sigma - (\gamma_\sigma + \gamma_\phi)]}{\gamma_\sigma[(\gamma_\sigma + \gamma_\phi)^2 + 4\Delta_\sigma^2] + 8(\gamma_\sigma + \gamma_\phi)\Omega_\sigma^2}, \quad (4b)$$

with  $\Delta_\sigma = (\omega_\sigma - \omega_L)$  the detuning between the two-level system and the driving laser.

To model the detection process self-consistently, one can couple to this system a detector and study the observables through this detector rather than from the object itself. A method (the so-called ‘cascaded formalism’) has been developed in the early 90s [82, 83] to model this theoretically. Such a precaution avoids (or reveals) the subtle mistake of assuming that the emitted light retains all the attributes of the source when these are computed or measured separately. To

take the example of interest in our discussion, one can indeed observe (or compute) the spectral width of the two-level system in the Heitler regime, and find an ultra-bright and ultra-narrow component, and then observe (or compute) its antibunching and find an excellent antibunching. These constitute separate characterisations of the source, and until these are measured simultaneously, they cannot be assumed to exist simultaneously. Indeed, characterising the light through the detector—which by the very nature of its excitation is being subject to the both aspects of interest simultaneously—one finds that the detected light is either antibunched but not narrower than the source, or is spectrally narrow but then with a poor or no antibunching. This depends on the spectral width of the detector itself: if the detector has a large spectral width, it will not be sensitive to the supposedly narrow linewidth light that excites it. If the detector has a narrow spectral width, it will not be sensitive to its antibunching. Given the character of quantum mechanics, we conclude that the failure of a detector to simultaneously capture the narrow linewidth and the antibunching really means that these do not actually jointly exist.

In the following we will discuss and generalise a scheme which we have recently proposed [33] and that achieves such a joint narrow and antibunched emission, in the sense that a detector does collect its light with these two attributes intact. As we will focus on antibunching and spectral width, we can support our analysis of the detection process through a ‘sensor’ that acts as a filter for the emitted light [74]. Theoretically, this is included through the vanishing coupling of a bosonic field with annihilation operator  $a$  to the dynamics of the two-level system, by adding the Hamiltonian  $H_a = g(\sigma^\dagger a + a^\dagger \sigma)$  to equation (1) and then taking the limit  $g \rightarrow 0$ , which allows the dynamics of the two-level system to be independent from that of the sensor. The bandwidth of the sensor is given by its decay rate  $\Gamma$  and is included as an extra term  $(\Gamma/2)\mathcal{L}_a\rho$  in the master equation (2). For quantities such as populations, which would vanish with  $g \rightarrow 0$ , one should use instead the more complete but also heavier cascaded formalism, which we have shown is equivalent to the more lightweight sensor method as far as correlations are concerned [84]. The main point of this theoretical shortcut is that instead of considering the light emitted by a system, one can consider instead the filtered light and this is enough to describe the process of detection, as long as the detector would have the same spectral width as the filter. We will therefore be speaking of filtering for the light emitted by the two-level system, which should be understood as the effect of its detection from a detector with the corresponding bandwidth.

When the emission of the two-level system is filtered in frequency, the tails of the incoherent Lorentzian are trimmed out and this spoils the perfect antibunching, that arises from an interference between the coherent and incoherent components [33]. This is even more salient with detuning, when the two-level system is detuned from the laser. In this case, the incoherent part of the spectrum splits into two peaks at  $\omega_L \pm \Delta_\sigma$  that surround the coherent part at  $\omega_L$ . It is, then, even more evident that filtering in frequency breaks the balance between the incoherent and coherent fractions. Such an interference, that

yields the perfect antibunching can be restored simply by reinstating the original proportion, i.e. the perfect antibunching can be maintained after filtering by reducing the surplus of coherent emission that passes in its entirety through the filter, if the latter one is at resonance with the laser. This can be easily achieved since a coherent field can be scaled at will through interferences, in our case, destructive interferences. Our scheme thus consists of interfering at a beam splitter the light emitted by the two-level system with a coherent field  $\beta \equiv |\beta|e^{i\phi}$ , whose amplitude and phase need to be fixed adequately to provide the exact compensation. In this configuration, the Hamiltonian for our laser-corrected source becomes

$$H = H_\sigma + \Delta_a a^\dagger a - ir|\beta|(e^{i\phi} a^\dagger - e^{-i\phi} a) + gt(\sigma^\dagger a + a^\dagger \sigma), \quad (5)$$

where  $H_\sigma$  is the Hamiltonian in equation (1),  $t$  and  $r$  are the transmission and reflection coefficients of the beam splitter (the reflection coefficient is preceded by a factor  $i$ , which accounts for the phase shift gained by the reflection in the beam splitter), and  $\Delta_a = (\omega_a - \omega_L)$  is the detuning between the detector and the driving laser. The amplitude of the coherent field  $|\beta|$  can be parameterised as a fraction  $\mathcal{F}$  of the coherent field that the sensor receives from the two-level system, i.e. we may write

$$|\beta| = g \frac{\Omega_\sigma t}{\gamma_\sigma r} \mathcal{F}, \quad \text{or equivalently} \quad |\beta'| = g \frac{\Omega_\sigma}{\gamma_\sigma} \mathcal{F}, \quad (6)$$

where we have also defined  $|\beta'| = |\beta|(r/t)$ , to avoid carrying the parameters of the beam splitter, which only renormalize the observables but do not change the physics involved. With these definitions we can now compute any observable in the steady-state to leading order in  $\Omega_\sigma$ , such as the total intensity detected by the sensor (its population):

$$n_a = \langle a^\dagger a \rangle = \frac{4g^2 t^2 \Omega_\sigma^2 [4\gamma_\sigma^2 + \mathcal{F}^2(\gamma_\sigma^2 + 4\Delta_a^2) + 4\gamma_\sigma \mathcal{F}(\gamma_\sigma \cos \phi - 2\Delta_a \sin \phi)]}{\gamma_\sigma(\Gamma^2 + 4\Delta_a^2)(\gamma_\sigma^2 + 4\Delta_a^2)}. \quad (7)$$

Although this is not immediately apparent from the analytical expression (7), the scheme leads to a decrease of the single-photon repetition rate, which is the price to pay to combine strong antibunching with subnatural-linewidth emission. This can be well understood as the destructive interference removing the detrimental excess of coherent signal. The quantum signal is of greater quality, but in a smaller quantity.

As a final note, we observe that the interference between the incoherent and coherent fractions, responsible for the perfect antibunching, takes place regardless of the detuning between the laser and the two-level system. That is to say, the interference takes place even when there would seem to have no spectral overlap between the two fractions, that can be arbitrarily separated. This is another manifestation of the misconception of a quantum quantity existing without being observed. Namely, without frequency-resolved detection, the measurement does consider that all the photons are identical, being completely blind to their frequency, so it is mistaken to assume that their detuning leads to no spectral overlap. When the spectral properties of the photons are included, so that one can indeed evidence the spectral separation of the coherent

and incoherent fractions, their joint presence within the detector bandwidth indeed becomes key, as we show in what follows.

### 3. Results

The two-photon correlations detected in various spectral widths are obtained from the steady-state solution of the master equation (2) with  $H_\sigma$  replaced by the Hamiltonian in equation (5) and with the added Lindblad term  $(\Gamma/2)\mathcal{L}_a\rho$ . Although these correlations can be obtained in closed-form, they are too cumbersome to be written here. Instead, we will provide the particular cases (i) with detuning but no dephasing and (ii) at resonance but with dephasing. The full case, of which we will show one case graphically, brings little more insights, so treating these separately is enough to reach general conclusions. We consider first the case without dephasing.

#### 3.1. No dephasing

In the case of no dephasing, but allowing for some detuning, either between the driving laser and the two-level system or between the detector and the two-level system (or both), the detected two-photon correlations are given by, to leading order in the driving strength:

$$g_a^{(2)} = \langle a^\dagger 2a^2 \rangle / \langle a^\dagger a \rangle^2 = \tilde{\Gamma}_\sigma^2 (16\gamma_\sigma^4 + 16\mathcal{F}^2\gamma_\sigma^2\tilde{\Gamma}_+^2 + \mathcal{F}^4\tilde{\Gamma}_\sigma^2\tilde{\Gamma}_+^2 - 8\mathcal{F}\gamma_\sigma \{2(4\gamma_\sigma^2\Delta_+ + \mathcal{F}^2\Delta_\sigma\tilde{\Gamma}_+)\sin\phi + 2\gamma_\sigma\mathcal{F}(\gamma_+\Delta_\sigma + \gamma_\sigma\Delta_+)\sin 2\phi - \gamma_\sigma(4\gamma_\sigma\gamma_+ + \mathcal{F}^2\tilde{\Gamma}_+^2)\cos\phi - \gamma_\sigma\mathcal{F}(\gamma_\sigma\gamma_+ - 4\Delta_\sigma\Delta_+)\cos 2\phi\}) / (\tilde{\Gamma}_+^2 [4\gamma_\sigma^2 + \mathcal{F}^2\tilde{\Gamma}_\sigma + 4\gamma_\sigma\mathcal{F}(\gamma_\sigma\cos\phi - 2\Delta_\sigma\sin\phi)]^2), \quad (8)$$

where we have defined  $\gamma_+ \equiv \gamma_\sigma + \Gamma$ ,  $\Delta_+ \equiv \Delta_\sigma + \Delta_a$  and  $\tilde{\Gamma}_c^2 \equiv \gamma_c^2 + 4\Delta_c^2$  for  $c = \sigma, +$ . From this expression, it is easy to find particular cases of interest: perfect antibunching, when the numerator becomes zero, and perfect superbunching, when the denominator becomes zero.

The condition to vanish the numerator, and therefore to produce perfect antibunching, is given by

$$\mathcal{F} = -\frac{2\gamma_\sigma e^{-i\phi}}{\gamma_\sigma + 2i\Delta_\sigma} \left( 1 \pm \sqrt{\frac{\Gamma + 2i\Delta_a}{\Gamma_+ + 2i\Delta_+}} \right), \quad (9)$$

which generalizes the expression given in equation (10) of [33]. Since a real phase  $\phi$  can always be found so that equation (9) is a real positive number, the condition for perfect antibunching is always satisfied. The condition that cancels equation (8) also yields the suppression of the state with two photons in the detector, as we show in the appendix through a wave-function approximation. In the most natural configuration where the laser is resonant to both the sensor and the two-level system, equation (9) reduces to the

expressions of [33]:

$$\mathcal{F}_{2,\pm} = 2 \left( 1 \pm \sqrt{\frac{\Gamma}{\Gamma + \gamma_\sigma}} \right) \quad \text{and} \quad \phi_\pm = \pi. \quad (10)$$

On the other hand, the denominator of equation (8), that is, the intensity of the total signal  $\langle a^\dagger a \rangle$ , vanishes when one sets the phase  $\phi$  and amplitude  $\mathcal{F}$  of the interfering laser to satisfy

$$\tan\phi = -\frac{2\Delta_\sigma}{\gamma_\sigma} \quad \text{and} \quad \mathcal{F} = -2\cos\phi. \quad (11)$$

Note that unlike for antibunching, this condition to obtain superbunching is independent of the detector properties, both frequency and resolution. The reason is that it is always possible for the external laser to suppress completely the coherent fraction, which in this case dominates the total intensity, through destructive interference. This happens already at the beam splitter, regardless of the detector properties. It is only a matter of adjusting the phase and intensity of the external laser. In this case,  $g_a^{(2)}$  diverges (to first order in the driving strength, so that higher order terms would produce huge but finite values of  $g_a^{(2)}(0)$ ). Such a strong superbunching corresponds to the statistics of the quantum fluctuations, which are the only signal that remains when fully removing the coherently scattered fractions. The incoherent part of the signal is wildly fluctuating and even has notable squeezing properties, that are discussed elsewhere [85]. Therefore, photon emission is not occurring in the form of photon bundles and cannot be Purcell-enhanced, so that prospects for applications as  $N$ -photon sources are limited. Also, we mention that infinite bunching has already been reported before; it occurs for instance with Fock states in bosonic cascades [86].

A full map of  $g_a^{(2)}(0)$  as defined by equation (8) is shown in figures 1(a)–(c) for spectral widths of the detector ranging from essentially full-bandwidth, panel (a), the linewidth of the two-level system, panel (b) and with sub-linewidth resolution, panel (c). In the first case, without frequency filtering, perfect antibunching is obtained without any laser correction, that is, for  $\mathcal{F} = 0$  and independently of the phase. This corresponds to the case considered in the literature [76, 77], but this comes at the cost of the spectral width: the  $\delta$ -width of the laser is completely washed out by the detector. For a detector spectrally matched to the emitter, shown in (b), antibunching is considerably reduced by the detector (to  $g_a^{(2)}(0) \approx 0.25$ ). Keeping the same linewidth, antibunching can be restored by the interfering laser fulfilling conditions (10), restoring an exact antibunching,  $g_a^{(2)}(0) = 0$ , to first order in the driving. Going to sub-natural linewidth with a detector spectrally matched to  $0.2\gamma_\sigma$ , shown in panel (c), one finds that antibunching is now almost completely gone in absence of the laser correction,  $g_a^{(2)}(0) \approx 0.7$ , but can again be fully restored with the laser correction. In all cases, in between the two conditions for antibunching, one can see the superbunching at  $\mathcal{F} = 2$ . Note that, as the linewidth is made narrower, the conditions for antibunching, equation (10), come closer to the conditions for superbunching, equation (11). So while this effect could be pursued down to extremely narrow linewidths,

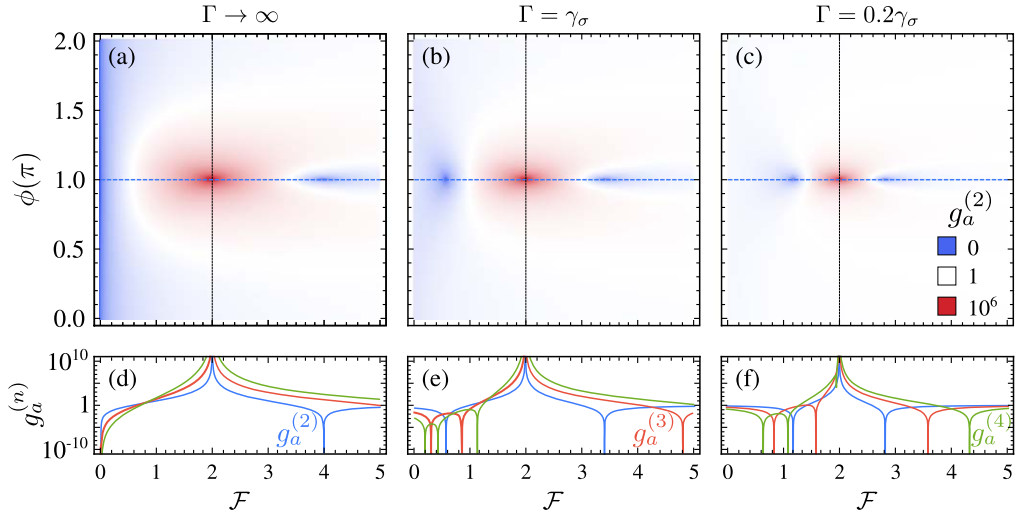


**Figure 1.** Filtered two-photon correlations at resonance and without dephasing, as a function of the parameters  $\mathcal{F}$  (intensity) and  $\phi$  (phase) of a superimposed interfering laser. In all the panels we set  $\gamma_\sigma$  as the unit,  $\Delta_\sigma = \Delta_a = 0$  and  $\gamma_\phi = 0$ . The detector linewidth decreases in from (a)–(c) as indicated on each panel.

at no cost for the antibunching, some restrictions would arise from the stability of the driving laser, as energy fluctuations would take the system from the condition for perfect antibunching to the condition for superbunching. Panels (d)–(f) show in blue lines transverse cuts at  $\phi = \pi$  of panels (a)–(c), and in red and green lines the corresponding higher-order correlators  $g_a^{(3)}$  and  $g_a^{(4)}$ , respectively. This shows how, although both  $\mathcal{F}_{2,\pm}$  from equation (10) yield an exact cancellation of  $g_a^{(2)}$ , the higher order correlations remain sub-Poissonian in the vicinity of only  $\mathcal{F}_{2,-}$  (which corresponds to the condition to obtain a ‘conventional antibunching’ [85]).

### 3.2. Dephasing

We now turn to the impact of dephasing, which is detrimental to photon correlations, but can still be corrected to a considerable extent through our process, although not perfectly anymore. In the case of dephasing alone, where both the two-level system and the detector are resonant with the driving laser, the two-photon correlations are given by

$$\begin{aligned}
 g_a^{(2)} = & \Gamma_\phi(\Gamma + \Gamma_\phi)(16\gamma_\sigma^3(\Gamma + \gamma_+)(2\Gamma + \gamma_+) \\
 & + 16\mathcal{F}^2\gamma_\sigma\gamma_+^2(2\Gamma + \Gamma_\phi)(3\Gamma + \Gamma_\phi) \\
 & + \mathcal{F}^4\gamma_+\Gamma_\phi(\Gamma + \Gamma_\phi)(2\Gamma + \Gamma_\phi)(3\Gamma + \Gamma_\phi) \\
 & + 8\mathcal{F}\gamma_\sigma\gamma_+(3\Gamma + \Gamma_\phi)\{\mathcal{F}\gamma_\sigma(2\Gamma + \Gamma_\phi)\cos 2\phi \\
 & + [4\gamma_\sigma(\Gamma + \gamma_+) + \mathcal{F}^2(\Gamma + \Gamma_\phi)(2\Gamma + \Gamma_\phi)]\cos \phi\}) / \\
 & \{\gamma_+^2(2\Gamma + \Gamma_\phi)(3\Gamma + \Gamma_\phi) \\
 & \times [(4 + \mathcal{F}^2)\gamma_\sigma\gamma_+ + \mathcal{F}^2\gamma_\phi(\gamma_+ + \Gamma_\phi) \\
 & + 4\mathcal{F}\gamma_\sigma(\Gamma + \Gamma_\phi)\cos \phi]^2\},
 \end{aligned} \tag{12}$$

where we have used the notation  $\Gamma_\phi = \gamma_\sigma + \gamma_\phi$  and  $\gamma_+ = \gamma_\sigma + \Gamma$ .

The general case that also includes detuning is shown in figure 2. In this case, the laser is detuned from the two-level system, while the detector is set either at the frequency of the two-level system (panels (a) and (c)) or at the frequency of the laser (panels (b) and (d)). The top row of figure 2 is given by equation (8) while the bottom row, for which a closed-form expression exists but is too bulky to be written here, is only shown graphically. The filter linewidth, or, equivalently, the bandwidth of the detector, has been taken to match one fifth of the emitter linewidth. Therefore, figures 2(a) and (b) are the detuned versions of figure 1(c). Using this panel as a reference, one can see the impact of dephasing (spoiling the correlations) and detuning (maintained but for different laser corrections). Actually, the condition for superbunching is independent from the detuning between the detector and the driving laser, in agreement with equation (11), unlike the condition for antibunching. In fact, when the detector is resonant to the laser, both being detuned from the emitter, the conditions for perfect antibunching do not occur at the same phase  $\phi$ . Therefore, in a detuned measurement, the correlations are easier to observe when the sensor is resonant to the two-level system.

While in absence of dephasing (equation (8)), correlations can range from exactly zero to infinity, equation (12) shows that in its presence, they can only be pushed to finite values, both for bunching and antibunching. Although the full expressions for those limiting values can be found, they are too bulky to be written here and are instead plotted in figures 2(e) and (f), respectively. The loss of antibunching due to dephasing cannot be compensated exactly by the interfering laser up to the point where, for strong enough dephasing, no antibunching at all can be maintained. Nevertheless, the laser correction still brings considerable improvement on the case without interference, which is also, of course, affected by dephasing. The intensity  $\mathcal{F}$  that yields the best antibunching

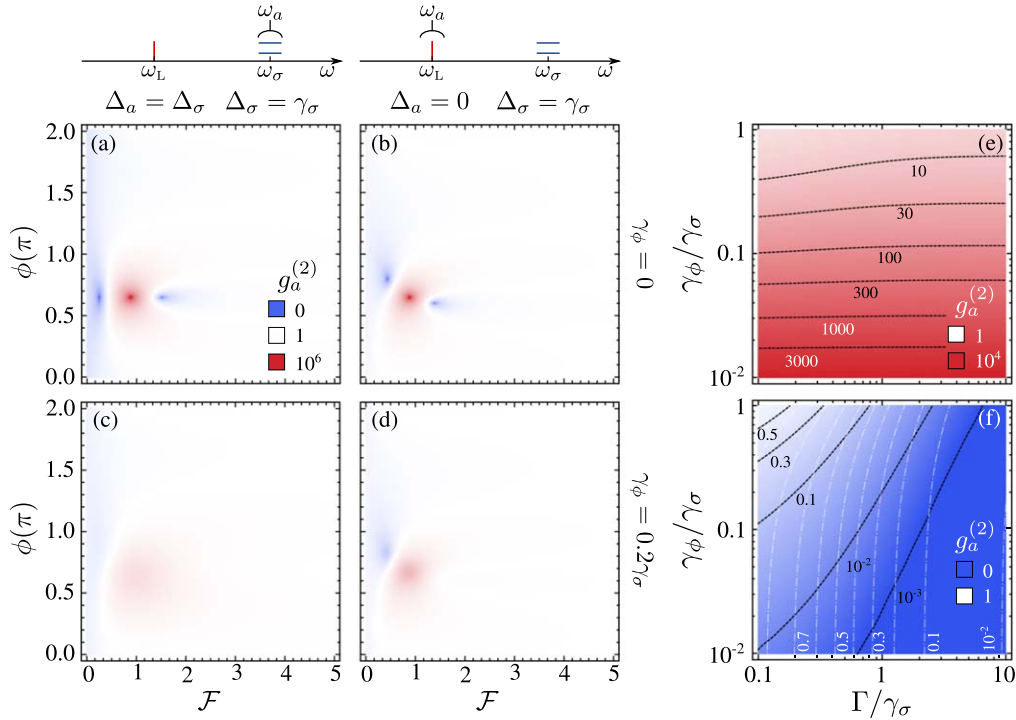


**Figure 2.** (a)–(d) Two-photon correlations as a function of the parameters of the interfering laser when the laser is detuned from the two-level system, in absence (top row) and in presence (bottom row) of dephasing. In the left column, the detector is resonant to the emitter while in the right column, it is to the driving laser. Dephasing spoils the perfect antibunching, and it is particularly detrimental in the case where the sensor is set in resonance the two-level system, in which case the dephased correlations are completely blurred. Without dephasing, one may still find the condition for  $\mathcal{F}$  that provides perfect antibunching. In panels (a)–(d) we set  $\Gamma = \gamma_\sigma/5$ . (e), (f) Maximum and minimum value of  $g_a^{(2)}$  when the two-level system, the sensor and the laser are in resonance. Namely, for each dephasing  $\gamma_\phi$  and sensor linewidth  $\Gamma$ , we optimize the correlation in equation (12) over all the values of the intensity and the phase of the external laser  $\mathcal{F}$  and  $\phi$ , respectively. In panel (f) we also show in dashed-dotted white lines the isolines for the minimum correlations that can be obtained without the correction (i.e. with  $\mathcal{F} = 0$ ).

is found by minimising equation (12), which does not provide a simple closed-form expression, but can be readily found numerically. The minimum antibunching obtained this way is shown in figure 2(f).

As in the case without dephasing, superbunching is found for particular interference conditions:

$$\mathcal{F} = \frac{2\gamma_\sigma}{\sqrt{\Gamma_\phi^2 + 4\Delta_\sigma^2}} \quad \text{and} \quad \tan \phi = -\frac{2\Delta_\sigma}{\Gamma_\phi}, \quad (13)$$

which are independent of the detector properties (detuning and bandwidth). These correspond, again, to the complete suppression of the coherent fraction ( $\langle a \rangle = 0$ ), but, this time, not of the total signal  $n_a$ , which now also has some incoherent component to leading-order in  $\Omega_\sigma$ . The conditions for superbunching are independent of the detector properties for the same reason as in the case without dephasing, but now the value of superbunching does depend on both of the detector properties,  $\Delta_a$  and  $\Gamma$ , as shown in figure 2(e). In general, frequency filtering deeply affects the statistics of any signal and, in this case, of quantum fluctuations (the incoherent component). Since we have fully removed the coherent part, one can check that quantum fluctuations behave as any incoherently pumped source, fulfilling  $\lim_{\Gamma \rightarrow 0} g_a^{(2)} = 2$  [74].

### 3.3. Correlations in time

While the value of the zero-delay correlation between photons is usually the one considered to quantify the sub-Poissonian character of a source, the correlations between photons detected with a time difference  $\tau$  are also important. In particular, fast oscillations in correlations can be difficult to resolve and average out the result. In [33], we showed that in the case without dephasing and in resonance, when the loss of antibunching due to filtering is corrected with an external laser, the  $g_a^{(2)}(\tau)$  displays a plateau of perfectly antibunched photons for up to  $|\tau| \approx 2.5/\gamma_\sigma$ . This actually confers to such sources an even greater single-photon source character. As can be expected, correlations in time are affected by dephasing as well as by the detuning between the two-level system, the sensor and the laser. Such a characteristic profile is shown as filled blue lines in figure 3, to which we compare the cases treated in this text. Panels (a) and (b) show the effect of detuning (without dephasing) and Panel (c) shows the effect of dephasing (without detuning). In (a) the detector is resonant with the two-level system, and both are detuned from the driving laser, while in (b), the detector is resonant with the laser, and both are detuned from the emitter. In green lines are shown the correlations for the given parameters featured in inset while red lines show the result without the laser correction, i.e. with  $\mathcal{F} = 0$ .

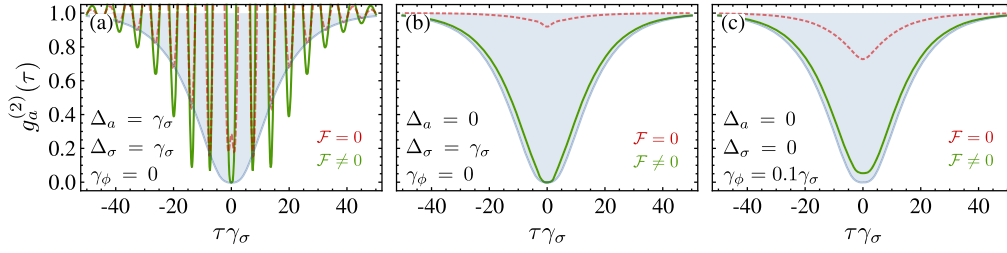


**Figure 3.** Time-resolved filtered two-photon correlations in the various configurations discussed in the text. The filled-blue line is the case at resonance and without dephasing. Panels (a) and (b) show the impact of various detunings without dephasing and Panel (c) shows the impact of dephasing at resonance. In green the best correction that can be achieved with an interfering laser, in red the uncorrected case. In all cases  $\Gamma = \gamma_\sigma/5$ .

Remarkably, the case where the detector is detuned from the laser, figure 3(a), displays fast oscillations with a frequency given by the detuning  $\Delta_a$ . The lower bound of the oscillations is approximately given by the aforementioned antibunching plateau and the zero delay correlations are still compensated exactly (as previously discussed), but the plateau itself becomes tainted. This means that, although the configuration with the detector in resonance to the emitter could seem the more natural or appealing one, the fast oscillations in its delay correlations makes it potentially problematic. Even when the driving laser is at resonance with the emitter, oscillations occur if the detector is somewhere else. In order to avoid them, detection should be done, in this case, at the frequency of the laser. These oscillations are unrelated to the specific physics described in this manuscript but are a general beating feature of any dynamics that involves several frequencies. For instance, looking at the correlations from a simple harmonic mode under incoherent thermal driving, and setting the detector out of resonance, we find oscillations in the second order coherence function and other correlators. Such oscillations dominate the temporal correlations whenever one detects light out of resonance from the spectral peaks, whatever source is being considered. Conversely, when the detector is resonant to the laser, panel (b), the plateau of antibunching is still present, albeit for a shorter time, and the correlations do not display any oscillations. It is also shown how the laser-correction makes a huge improvement on the antibunching as compared to the standard case which features almost no antibunching. However, a very large detuning between the two-level system and the laser (not shown) washes out the plateau and the correlations become simply  $g_a^{(2)}(\tau) = (1 - e^{-\Gamma\tau/2})^2$ , which corresponds to the correlations of a two-level system of linewidth  $\Gamma$  driven incoherently in the regime of low excitation.

In figure 3(c), it is shown how the zero-delay correlation of the dephased two-level system *cannot* be compensated exactly in presence of dephasing, as already stated, but otherwise suffers little in term of its plateau or coherence time. More importantly, it remains largely improved as compared to the case without the interference, with a value of  $g_a^{(2)}(0) \approx 0.05$  for a dephasing rate of 10% the emitter decay rate, whereas it is only  $g_a^{(2)}(0) \approx 0.73$  without the laser

correction. Furthermore, the measured linewidth remains well below the natural (but broadened by the dephasing) linewidth of the two-level system.

### 3.4. Performance of the laser-corrected subnatural-linewidth single-photon source

Further to the zero-delay correlation between photons, one can classify single-photon sources through their suppression of multi-photon emission at *all* orders, rather than only the second-order one [87]. This allows to classify and compare a wide range of sources beyond their mere  $g^{(2)}$  and thus avoiding that a squeezed state, that can have high probability of three-photon emission, appears to be a better single-photon source than a two-level system. Namely, we classify single-photon sources by their minimizing the ‘ $N$ -norm’ of all the  $j$ th order correlations up to  $j = N + 1$  [87]:

$$\|g_a^{(k)}\|_N = \left( \sum_{j=2}^{N+1} g_a^{(j)N} \right)^{1/N}. \quad (14)$$

An insightful parameter for comparison is the linewidth  $\Gamma$  of the detector. Indeed, in the ideal case  $\Gamma \rightarrow \infty$ , many sources trivially exhibit an exact  $\|g_a^{(k)}\|_N = 0$  and thus cannot be discriminated, while this can be done through their asymptotic behaviour towards this limit. Furthermore, since in a realistic setup, one deals with a finite-bandwidth detector, it is interesting to see the evolution of this criterion as a function of  $\Gamma$ . For our source in particular, which chief quality is its sub-natural linewidth, it becomes important to assess whether it still performs well in this regime. We will see that it is indeed the best source.

Although the criterion in equation (14) requires the computation of the photon correlation to all orders, oftentimes the  $N$ -norm converges for  $N \approx 3$  (i.e. requiring up to  $g_a^{(4)}$ ). In figure 4 we use the ‘3-norm’ ( $\|g_a^{(k)}\|_3$ ) to compare the behaviour of our laser-corrected subnatural-linewidth source (solid blue line) to the epitome of single-photon sources: a two-level system driven either with an incoherent pump (solid red line) or with a coherent pump in the Heitler regime (solid green line). As is well known, the coherent driving provides better single-photon source performances than its incoherent counterpart. Our scheme, thanks to its combined multi-photon suppression and sub-linewidth emission, greatly outperforms

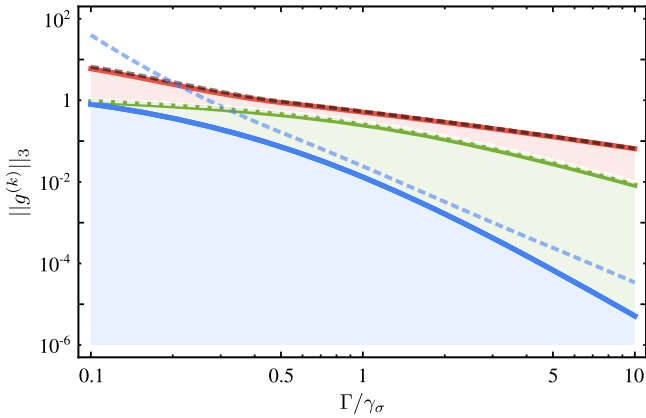


**Figure 4.** Comparison among single-photon sources using the 3-norm. While the two-level system driven coherently in the Heitler regime (solid green) outperforms the two-level system driven incoherently (solid red) across all the values of  $\Gamma/\gamma_\sigma$ , our laser-corrected source (solid blue) is the best of the three down to  $\Gamma/\gamma_\sigma \approx 0.1$ . The effect of the dephasing to the two-level system leave the ‘bare’ two-level systems unchanged, both under coherent (dashed white) and incoherent (dashed black) driving. However, the same dephasing rate spoils notably our laser-corrected source (dashed blue). The figure was obtained in the regime of vanishing driving: (i)  $P_\sigma \ll \gamma_\sigma$  for the two-level system driven incoherently and (ii)  $\Omega_\sigma \ll \gamma_\sigma$  for the two-level system driven coherently and for the laser-corrected source. The cases with dephasing were obtained with  $\gamma_\phi = 0.2\gamma_\sigma$ .

the two-level system in both regimes, by several orders of magnitude in the region of  $\Gamma \gtrsim \gamma_\sigma$  and retains its advantage down to about  $\Gamma \gtrsim \gamma_\sigma/5$ , according to this criterion. It remains in fact a much better single-photon source according to  $g^{(2)}$  alone, as the Heitler antibunching does not survive sub-linewidth filtering [33]. However, in the stricter sense of suppressing all-order correlations, the laser-corrected source gets spoiled due to high three-photon bunching [33] when filtering is too narrow. Overall, the laser-corrected source thus proves to be the best single-photon source known to date down to a linewidth a fifth of the radiative linewidth of the original two-level system.

We conclude with the impact of dephasing on the performance of this optimum source. We have already commented how, the scheme relying on an interference effect with a coherent (well-defined phase) field, it is particularly sensitive to dephasing. The 3-norm criterion is severe in this regard, as seen in figure 4, where the impact of 20% dephasing rate ( $\gamma_\phi = \gamma_\sigma/5$ ) is shown as dashed lines for all the three types of source. The dephasing hardly worsens the conventional schemes’ ability to suppress multi-photon emission (dashed black and dashed white lines on top of the solid red and solid green lines, respectively). Conversely, the same dephasing rate affects notably the behaviour of the laser-corrected source, although even for  $\Gamma/\gamma_\sigma$  as small as 0.3, the source performs better than the two-level systems. Therefore, while it is much more fragile to dephasing, its performance is so much greater than other schemes that it still

remains superior to them over the ranges of greatest relevance and interest.

#### 4. Conclusions

We study the laser-corrected scheme that produces joint antibunching and subnatural linewidth emission [33]. Not only does this scheme make these properties hold simultaneously, it also produces perfect antibunching to first order in the driving (that is,  $g_a^{(2)}(0) = 0$ ) which is otherwise possible only by integrating all frequencies, and features a plateau in the time-delayed photon correlations, making such a single-photon source more effective at suppressing coincidences. Its performance has been further demonstrated by turning to a stricter criterion to quantify single-photon sources, taking into account photon correlations of higher orders. This allows us to compare it to a wide class of single-photon sources with the result that the laser-corrected source outperforms the others by several orders of magnitudes for detectors’ linewidth larger than the radiative linewidth of the two-level system, and still remains the best one in the subnatural linewidth regime. There, according to the 3-norm criterion, its superiority as compared to simple resonance fluorescence is less compelling, but this is due to a large three-photon component, on top of still perfect two-photon antibunching, while resonance fluorescence in turn is spoiled already at the two-photon level. We have also shown that different conditions from the interfering laser produce instead perfect superbunching (that is,  $g_a^{(2)}(0) = \infty$  to first order in the driving).

We have specifically considered the presence of dephasing and of a detuning from the emitter with either the driving laser and/or the detector. In presence of detuning, we find that perfect antibunching can always be enforced by the interference, but with strong time oscillations of the statistics when the detector is detuned from the driving laser. These oscillations disappear when the detection is made at the frequency of the laser, hence favouring this configuration. In the presence of dephasing, which one can expect to be particularly detrimental since the scheme relies on an interference with a coherent source of well-defined phase, we confirm that antibunching is significantly spoiled and only finite values can be obtained. However, the improvement as compared to the non-corrected single-photon source is so great in the first place as to be able to still withstand the very detrimental effects of dephasing. Multi-photon suppression remains better than from two-level systems under either coherent or incoherent driving for detectors with linewidth down to  $\Gamma \approx 0.3\gamma_\sigma$ . This makes the laser-corrected single-photon source the best cw scheme known to date.

#### Acknowledgments

Funding from the joint Russian-Greek project RFME-FI61617X0085 supported by the Ministry of Science and

Education of the Russian Federation, the Universidad Autónoma de Madrid under contract FPI-UAM 2016, the Spanish MINECO under contract FIS2015-64951-R (CLAUQUE) & the RyC program is gratefully acknowledged.

## Appendix. Wavefunction approximation method at vanishing pumping regime

In the context of this work, the wavefunction approximations [88] consist of assuming that the state of the system composed by two fields, with annihilation operators  $\xi$  and  $c$  following either pseudo-spin or bosonic algebra, can be approximated by a pure state, which reads in the Fock state basis

$$|\psi\rangle = \sum_{n,m} C_{nm} |n\rangle_c |m\rangle_\xi \equiv \sum_{n,m} C_{nm} |n, m\rangle, \quad (\text{A.1})$$

where  $C_{nm}$  are the probability amplitude of having  $m$  photons in the field of operator  $\xi$  and  $n$  photons in the field of operator  $c$ . The summation extends over the boundaries of the respective spaces, which is 1 for a two-level system and  $\infty$  for a bosonic one, which in practice is truncated to  $N$ . Since the dynamics of the system is given by the master equation

$$\partial_t \rho = i[\rho, H] + \sum_k (\tilde{\Gamma}_k/2) \mathcal{L}_{j_k} \rho, \quad (\text{A.2})$$

where  $H$  is the Hamiltonian of the system and assuming the dissipation in the form of ‘jump operators’  $j_k$  at rates  $\tilde{\Gamma}_k$ , the dynamics of the wavefunction is given by Schrödinger equation

$$\partial_t |\psi\rangle = -iH_{\text{eff}} |\psi\rangle, \quad (\text{A.3})$$

where  $H_{\text{eff}}$  is a non-hermitian Hamiltonian constructed as  $H_{\text{eff}} = H - i\sum_k \tilde{\Gamma}_k j_k^\dagger j_k$ , and the coefficients evolve as

$$\partial_t C_{nm} = -i\sum_{p,q} \langle n, m | H_{\text{eff}} | p, q \rangle C_{pq}. \quad (\text{A.4})$$

In our particular case, in which we describe the excitation of a sensor (a harmonic oscillator) by the emission of a two-level system, which in turn is driven in the Heitler regime by a laser, the Hamiltonian is the one given in equation (5) of the main text:

$$H = \Delta_\sigma \sigma^\dagger \sigma + \Delta_a a^\dagger a + \Omega_\sigma (\sigma^\dagger + \sigma) + gt(\sigma^\dagger a + a^\dagger \sigma) - ir|\beta|(a^\dagger e^{i\phi} - a e^{-i\phi}). \quad (\text{A.5})$$

Here the two-level system is driven with intensity  $\Omega_\sigma$  and is coupled to the sensor with strength  $g$ , the sensor is also driven by a field  $\beta e^{i\phi}$  and the detuning between the two-level system (resp. sensor) and the driving laser is given by  $\Delta_\sigma$  (resp.  $\Delta_a$ ). These fields are attenuated by the transmission  $t$  and reflection  $r$  coefficients of the beam splitter in which they interfere. Considering that the two-level system and the sensor have decay rates  $\gamma_\sigma$  and  $\Gamma$ , respectively, the effective Hamiltonian that describes the dynamics in the

wavefunction approximation reads<sup>4</sup>

$$H_{\text{eff}} = H - \frac{i}{2}(\gamma_\sigma \sigma^\dagger \sigma + \Gamma a^\dagger a), \quad (\text{A.6})$$

where  $H$  is the Hamiltonian in equation (A.5). Replacing the effective Hamiltonian in equation (A.6) in the expression in equation (A.3), we obtain the differential equations for the coefficients of interest:

$$i\partial_t C_{01} = \Omega_\sigma + gtC_{10} + ir|\beta| e^{-i\phi} C_{11} + \left(\Delta_\sigma - i\frac{\gamma_\sigma}{2}\right) C_{01}, \quad (\text{A.7})$$

$$i\partial_t C_{10} = -ir|\beta| e^{i\phi} + \Omega_\sigma C_{11} + gtC_{01} + \sqrt{2}ir|\beta| e^{-i\phi} C_{20} + \left(\Delta_a - i\frac{\Gamma}{2}\right) C_{10}, \quad (\text{A.8})$$

$$i\partial_t C_{11} = \Omega_\sigma C_{10} - ir|\beta| e^{i\phi} C_{01} + \sqrt{2}gtC_{20} + \left(\Delta_\sigma + \Delta_a - i\frac{\gamma_\sigma + \Gamma}{2}\right) C_{11}, \quad (\text{A.9})$$

$$i\partial_t C_{20} = \sqrt{2}gtC_{11} - \sqrt{2}ir|\beta| e^{i\phi} C_{10} + 2\left(\Delta_a - i\frac{\Gamma}{2}\right) C_{20}, \quad (\text{A.10})$$

where we have assumed that the driving to the two-level system is low enough so that the states with three or more excitations can be safely neglected, and that the driving laser is resonant to both the two-level system and the sensor. Assuming that the coherent field that drives the sensor can be written as a fraction of the field that drives the two-level system, as in equation (6), and to leading order in the coupling and the driving intensity of the two-level system, the solution to equations (A.7)–(A.10) is

$$C_{01} = -\frac{2i\Omega_\sigma}{\gamma_\sigma + 2i\Delta_\sigma}, \quad (\text{A.11})$$

$$C_{10} = -\frac{2gt\Omega_\sigma[2\gamma_\sigma + (\gamma_\sigma + 2i\Delta_\sigma)\mathcal{F}e^{i\phi}]}{\gamma_\sigma(\Gamma + 2i\Delta_a)(\gamma_\sigma + 2i\Delta_\sigma)}, \quad (\text{A.12})$$

$$C_{11} = \frac{4igt\Omega_\sigma^2[2\gamma_\sigma + (\gamma_\sigma + 2i\Delta_\sigma)\mathcal{F}e^{i\phi}]}{\gamma_\sigma(\Gamma + 2i\Delta_a)(\gamma_\sigma + 2i\Delta_\sigma)(\gamma_\sigma + 2i\Delta_\sigma)}, \quad (\text{A.13})$$

$$C_{20} = \frac{2\sqrt{2}g^2t^2\Omega_\sigma^2\{4\gamma_\sigma^2 + (\gamma_\sigma + 2i\Delta_\sigma)e^{i\phi}\mathcal{F}[4\gamma_\sigma + e^{i\phi}\mathcal{F}(\gamma_\sigma + 2i\Delta_\sigma)]\}}{\gamma_\sigma^2(\Gamma + 2i\Delta_a)^2(\gamma_\sigma + 2i\Delta_\sigma)(\gamma_\sigma + 2i\Delta_\sigma)}. \quad (\text{A.14})$$

The population of both the two-level system and the sensor, as well as  $g_a^{(2)}$  can be obtained from the coefficients in equations (A.11)–(A.14) as  $n_a = |C_{10}|^2$ ,  $\langle n_\sigma \rangle = |C_{01}|^2$  and  $g_a^{(2)} = 2|C_{20}|^2/|C_{10}|^4$ , respectively. The cancellation of the coefficient  $C_{20}$ , and therefore of  $g_a^{(2)}$ , yields the condition on the attenuation factor

<sup>4</sup> The dephasing of the two-level system enters the description as an extra Lindblad term in the master equation:  $(\gamma_\phi/2)\mathcal{L}_{\sigma^\dagger\sigma}\rho$ , where  $\gamma_\phi$  is the rate of dephasing. However, the effect of this term is the decoherence of the state of the two-level system, which affects only the off-diagonal elements of the density matrix of the two-level system, and thus cannot be described through a wavefunction approximation.

$$\mathcal{F} = -\frac{2\gamma_\sigma e^{-i\phi}}{\gamma_\sigma + 2i\Delta_\sigma} \left( 1 \pm \sqrt{\frac{\Gamma + 2i\Delta_a}{\Gamma_+ + 2i\Delta_+}} \right), \quad (\text{A.15})$$

in agreement with equation (9) of the main text.

## ORCID iDs

J C López Carreño  <https://orcid.org/0000-0002-2134-0958>

E Zubizarreta Casalengua  <https://orcid.org/0000-0003-4967-595X>

F P Laussy  <https://orcid.org/0000-0002-1070-7128>

E del Valle  <https://orcid.org/0000-0002-0221-282X>

## References

- [1] Bennett C H and Brassard G 1984 Quantum cryptography: public key distribution and coin tossing *Proc. IEEE* **560** 175
- [2] Beveratos A *et al* 2002 Single photon quantum cryptography *Phys. Rev. Lett.* **89** 187901
- [3] Jennewein T, Simon C, Weihs G, Weinfurter H and Zeilinger A 2000 Quantum cryptography with entangled photons *Phys. Rev. Lett.* **84** 4729
- [4] Naik D S, Peterson C G, White A G, Berglund A J and Kwiat P G 2000 Entangled state quantum cryptography: eavesdropping on the Ekert protocol *Phys. Rev. Lett.* **84** 4733
- [5] Hu J-Y *et al* 2016 Experimental quantum secure direct communication with single photons *Light: Sci. App.* **5** e16144
- [6] Deutsch D *et al* 1996 Quantum privacy amplification and the security of quantum cryptography over noisy channels *Phys. Rev. Lett.* **77** 2818
- [7] Osorio C I *et al* 2012 Heralded photon amplification for quantum communication *Phys. Rev. A* **86** 023815
- [8] Zhou L and Sheng Y-B 2015 Recyclable amplification protocol for the single-photon entangled state *Laser Phys. Lett.* **12** 045203
- [9] Spring J B *et al* 2013 Boson sampling on a photonic chip *Science* **339** 798
- [10] Tillmann M *et al* 2013 Experimental boson sampling *Nat. Photon.* **7** 540
- [11] Broome M *et al* 2013 Photonic boson sampling in a tunable circuit *Science* **15** 794
- [12] Crespi A *et al* 2013 Integrated multimode interferometers with arbitrary designs for photonic boson sampling *Nat. Photon.* **7** 545
- [13] Loredó J C *et al* 2017 Boson sampling with single-photon Fock states from a bright solid-state source *Phys. Rev. Lett.* **118** 120503
- [14] Laucht A *et al* 2012 A waveguide-coupled on-chip single-photon source *Phys. Rev. X* **2** 011014
- [15] Schlehahn A *et al* 2018 A stand-alone fiber-coupled single-photon source *Sci. Rep.* **8** 1340
- [16] Krapick S *et al* 2013 An efficient integrated two-color source for heralded single photons *New J. Phys.* **15** 033010
- [17] Zadeh I E *et al* 2016 Deterministic integration of single photon sources in Silicon based photonic circuits *Nano Lett.* **16** 2289
- [18] Gazzano O *et al* 2012 Bright solid-state sources of indistinguishable single photons *Nat. Commun.* **4** 1425
- [19] Kim J-H, Cai T, Richardson C J K, Leavitt R P and Waks E 2016 Two-photon interference from a bright single-photon source at telecom wavelengths *Optica* **3** 577
- [20] Neergaard-Nielsen J S, Melholt Nielsen B, Takahashi H, Vistnes A I and Polzik E S 2007 High purity bright single photon source *Opt. Express* **15** 7940
- [21] Portalupi S L *et al* 2015 Bright phonon-tuned single-photon source *Nano Lett.* **15** 6290
- [22] Reimer M E *et al* 2012 Bright single-photon sources in bottom-up tailored nanowires *Nat. Comm.* **3** 737
- [23] Toishi M, Englund D, Faraon A and Vučković J 2009 High-brightness single photon source from a quantum dot in a directional-emission nanocavity *Opt. Express* **17** 14618
- [24] He Y-M *et al* 2017 Deterministic implementation of a bright, on-demand single-photon source with near-unity indistinguishability via quantum dot imaging *Optica* **4** 802
- [25] Santori C, Fattal D, Vučković J, Solomon G S and Yamamoto Y 2002 Indistinguishable photons from a single-photon device *Nature* **419** 594
- [26] He Y-M *et al* 2013 On-demand semiconductor single-photon source with near-unity indistinguishability *Nat. Nanotechnol.* **8** 213
- [27] Müller K *et al* 2016 Self-homodyne-enabled generation of indistinguishable photons *Optica* **3** 931
- [28] Na N and Yamamoto Y 2010 Massive parallel generation of indistinguishable single photons via the polaritonic superfluid to Mott-insulator quantum phase transition *New J. Phys.* **12** 123001
- [29] Dada A C *et al* 2016 Indistinguishable single photons with flexible electronic triggering *Optica* **3** 493
- [30] Ding X *et al* 2016 On-demand single photons with high extraction efficiency and near-unity indistinguishability from a resonantly driven quantum dot in a micropillar *Phys. Rev. Lett.* **116** 020401
- [31] Somaschi N *et al* 2016 Near-optimal single-photon sources in the solid state *Nat. Photon.* **10** 340
- [32] Khazali M, Heshami K and Simon C 2017 Single-photon source based on Rydberg excitation blockade *J. Phys. B: At. Mol. Phys.* **50** 215301
- [33] López Carreño J C, Zubizarreta Casalengua E, Laussy F P and del Valle E 2018 Joint subnatural-linewidth and single-photon emission from resonance fluorescence *Quantum Sci. Technol.* **3** 045001
- [34] Santana T S *et al* 2017 Generating indistinguishable photons from a quantum dot in a noisy environment *Phys. Rev. B* **95** 201410(R)
- [35] Verger A, Ciuti C and Carusotto I 2006 Polariton quantum blockade in a photonic dot *Phys. Rev. B* **73** 193306
- [36] Ridolfo A, Leib M, Savasta S and Hartmann M J 2012 Photon blockade in the ultrastrong coupling regime *Phys. Rev. Lett.* **109** 193602
- [37] Liew T C H and Savona V 2010 Single photons from coupled quantum modes *Phys. Rev. Lett.* **104** 183601
- [38] Gerace D and Savona V 2014 Unconventional photon blockade in doubly resonant microcavities with second-order nonlinearity *Phys. Rev. A* **89** 031803(R)
- [39] Flayac H, Gerace D and Savona V 2015 An all-silicon single-photon source by unconventional photon blockade *Sci. Rep.* **5** 11223
- [40] Muñoz-Matutano G *et al* 2017 Quantum-correlated photons from semiconductor cavity polaritons arXiv:1712.05551
- [41] Delteil A *et al* 2018 Quantum correlations of confined exciton-polaritons arXiv:1805.04020
- [42] Snijders H J *et al* 2018 Observation of the unconventional photon blockade *Phys. Rev. Lett.* **121** 043601
- [43] Vaneph C *et al* 2018 Observation of the unconventional photon blockade in the microwave domain *Phys. Rev. Lett.* **121** 043602
- [44] López Carreño J C, del Valle E and Laussy F P 2017 Photon correlations from the Mollow Triplet *Laser Photon. Rev.* **11** 1700090
- [45] Sánchez Muñoz C *et al* 2014 Emitters of N-photon bundles *Nat. Photon.* **8** 550

- [46] Sánchez Muñoz C, Laussy F P, del Valle E, Tejedor C and González-Tudela A 2018 Filtering multiphoton emission from state-of-the-art cavity quantum electrodynamics *Optica* **5** 14
- [47] Berquist W M I J C and Wineland D J 1988 Photon antibunching and sub-poissonian statistics from quantum jumps in one and two atoms *Phys. Rev. A* **38** 559
- [48] Grangier P, Roger G, Aspect A, Heidmann A and Reynaud S 1986 Observation of photon antibunching in phase-matched multiatom resonance fluorescence *Phys. Rev. Lett.* **67** 687
- [49] Rempe G, Schmidt-Kaler F and Walther H 1990 Observation of sub-poissonian photon statistics in a micromaser *Phys. Rev. Lett.* **64** 2783
- [50] Michler P *et al* 2000 A quantum dot single-photon turnstile device *Science* **290** 2282
- [51] Lounis B, Bechtel H A, Gerion D and Moerner P A W E 2000 Photon antibunching in single CdSe/ZnS quantum dot fluorescence *Chem. Phys. Lett.* **329** 399
- [52] Santori C, Pelton M, Solomon G, Dale Y and Yamamoto Y 2001 Triggered single photons from a quantum dot *Phys. Rev. Lett.* **86** 1502
- [53] Zwiller V *et al* 2001 Single quantum dots emit single photons at a time: Antibunching experiments *Appl. Phys. Lett.* **78** 2476
- [54] Sebald K *et al* 2002 Single-photon emission of CdSe quantum dots at temperatures up to 200 K *Appl. Phys. Lett.* **81** 2920
- [55] Pelton M *et al* 2002 Efficient source of single photons: a single quantum dot in a micropost microcavity *Phys. Rev. Lett.* **89** 2333602
- [56] Yuan Z *et al* 2002 Electrically driven single-photon source *Science* **295** 102
- [57] Gerardot B D *et al* 2005 Photon statistics from coupled quantum dots *Phys. Rev. Lett.* **95** 137403
- [58] Diedrich F and Walther H 1987 Nonclassical radiation of a single stored ion *Phys. Rev. Lett.* **58** 203
- [59] Bergquist J C, Hulet R G, Itano W M and Wineland D J 1986 Observation of quantum jumps in a single atom *Phys. Rev. Lett.* **57** 1699
- [60] Schubert M, Siemers I, Blatt R, Neuhauser W and Toschek P E 1992 Photon antibunching and non-poissonian fluorescence of a single three-level ion *Phys. Rev. Lett.* **68** 3016
- [61] Kask P, Piksarv P and Mets U 1985 Fluorescence correlation spectroscopy in the nanosecond time range: photon antibunching in dye fluorescence *Eur. Biophys. J.* **12** 163
- [62] Basché T, Moerner W E, Orrit M and Talon H 1992 Photon antibunching in the fluorescence of a single dye molecule trapped in a solid *Phys. Rev. Lett.* **69** 1516
- [63] Treussart F, Clouqueur A, Grossman C and Roch J-F 2001 Photon antibunching in the fluorescence of a single dye molecule in a thin polymer film *Opt. Lett.* **26** 1504
- [64] Lounis B and Moerner W E 2000 Single photons on demand from a single molecule at room temperature *Nature* **407** 491
- [65] Astafiev O *et al* 2010 Resonance fluorescence of a single artificial atom *Science* **327** 840
- [66] Bozyigit D *et al* 2011 Antibunching of microwave-frequency photons observed in correlation measurements using linear detectors *Nat. Phys.* **7** 154
- [67] Lang C *et al* 2013 Correlations, indistinguishability and entanglement in Hong-Ou-Mandel experiments at microwave frequencies *Nat. Phys.* **9** 345
- [68] Hoi I *et al* 2013 Microwave quantum optics with an artificial atom in one-dimensional open space *New J. Phys.* **15** 025011
- [69] Gu X, Kochum A F, Miranowicz C, Liu Y X and Nori F 2017 Microwave photonics with superconducting quantum circuits *Phys. Rep.* **718-719** 1
- [70] Kurtsiefer C, Mayer S, Zarda P and Weinfurter H 2000 Stable solid-state source of single photons *Phys. Rev. Lett.* **85** 290
- [71] Brouri R, Beveratos A, Poizat J-P and Grangier P 2000 Photon antibunching in the fluorescence of individual color centers in diamond *Opt. Lett.* **25** 1294
- [72] Messin G, Hermier J P, Giacobino E, Desbiolles P and Dahan M 2001 Bunching and antibunching in the fluorescence of semiconductor nanocrystals *Opt. Lett.* **23** 1891
- [73] del Valle E, Silva B, Muñoz C S, Carreño J C L and Laussy F 2018 Loss of antibunching In preparation
- [74] del Valle E, González-Tudela A, Laussy F P, Tejedor C and Hartmann M J 2012 Theory of frequency-filtered and time-resolved n-photon correlations *Phys. Rev. Lett.* **109** 183601
- [75] Heitler W 1944 *The Quantum Theory of Radiation* (Oxford: Oxford University Press)
- [76] Matthiesen C, Vamivakas A N and Atatüre M 2012 Subnatural linewidth single photons from a quantum dot *Phys. Rev. Lett.* **108** 093602
- [77] Nguyen H S *et al* 2011 Ultra-coherent single photon source *Appl. Phys. Lett.* **99** 261904
- [78] Vogel W 1995 Homodyne correlation measurements with weak local oscillators *Phys. Rev. A* **51** 4160
- [79] Collett M J, Loudon R and Gardiner C W 1987 Quantum theory of optical homodyne and heterodyne detection *J. Mod. Opt.* **34** 881
- [80] Fischer K A *et al* 2016 Self-homodyne measurement of a dynamic mollow triplet in the solid state *Nat. Photon.* **10** 163
- [81] Fischer K A *et al* 2017 On-chip architecture for self-homodyned nonclassical light *Phys. Rev. Appl.* **7** 044002
- [82] Gardiner C W 1993 Driving a quantum system with the output field from another driven quantum system *Phys. Rev. Lett.* **70** 2269
- [83] Carmichael H J 1993 Quantum trajectory theory for cascaded open systems *Phys. Rev. Lett.* **70** 2273
- [84] López Carreño J C, del Valle E and Laussy F P 2018 Frequency-resolved Monte Carlo *Sci. Rep.* **8** 6975
- [85] Zubizarreta Casalengua E, López Carreño J C, Laussy F and del Valle E 2018 Squeezing effect on the statistics of light-matter couplings in preparation
- [86] Liew T C H *et al* 2016 Quantum statistics of bosonic cascades *New J. Phys.* **18** 023041
- [87] López Carreño J C, Zubizarreta Casalengua E, del Valle E and Laussy F P 2016 Criterion for single photon sources arXiv:1610.06126
- [88] Visser P M and Nienhuis G 1995 Solution of quantum master equation in terms of a non-hermitian hamiltonian *Phys. Rev. A* **52** 4727